

Inflation from a chaotic potential with a step

Clara Rojas^{1,*} and Rafael Hernández-Jiménez^{2,†}

¹*Yachay Tech University, School of Physical Sciences and Nanotechnology, Hda. San José s/n y Proyecto Yachay, 100119, Urcuquí, Ecuador*

²*Departamento de Física, Centro Universitario de Ciencias Exactas e Ingeniería, Universidad de Guadalajara Av. Revolución 1500, Colonia Olímpica C.P. 44430, Guadalajara, Jalisco, México*

(Dated: June 16, 2022)

In this work we study the effects on relevant observational parameters of an inflationary universe from a chaotic potential with a step. We evolve numerically the perturbation equations within both cold and warm inflation. On the one hand, in a cold inflation scenario we analyse the scalar power spectrum $P_{\mathcal{R}}$ in terms of the number of e-folds N_e , and in terms of the ratio k/k_0 , where k_0 is our pivot scale. We show how $P_{\mathcal{R}}$ oscillates around $0.2 < k/k_0 < 20$. Also, we present the evolution of two relevant parameters: the scalar spectral index n_s and the tensor-to-scalar ratio r . Actually, more than one region of (n_s, r) lies within the observable window (Planck 2018). On the other hand, in the warm inflationary instance we present two examples, both related to previous samples. We examine the evolution of the scalar power spectrum in terms of N_e , where it can be observed a growth of its amplitude with respect to bigger k/k_0 . This result might imply that a warm step potential enhances the evolution of $P_{\mathcal{R}}$ at larger fluctuation scales. Finally, one key aspect of this research was to contrast the features of an inflationary potential between both paradigms; and in fact they show similarities and differences among various cases. One remarkable upshot in both scenarios is that certain fluctuation scales are no longer “freeze in” on super-horizon scales. Thus, this outcome might suggest that purely adiabatic primordial density perturbations no longer holds at the time of the step. Nonetheless, a deeper study is needed to assure that entropy production is indeed happening at super-horizon scales. And on the other hand, warm inflation could function as a screening mechanism capable of smoothing the feature of the inflationary potential.

PACS numbers: 98.80.Cq, 98.80.Jk

I. INTRODUCTION

The Standard Big Bang (SBB) paradigm describes successfully the evolution of the universe at large scales. This theory rests upon four fundamental pillars, a theoretical framework bases on general relativity, as put forward by Einstein and Friedman, and three robust observational facts: 1) the expansion of the universe observed by Hubble; 2) the observed abundance of light elements predicted by Gamow and his collaborators; and 3) the presence of the Cosmic Microwave Background (CMB) of a very isotropic black-body radiation at a temperature of about 3 K, which presents a high degree of uniformity with inhomogeneity of about one part in 10^5 [1]. Due to observation of the CMB by Penzias and Wilson, the SBB theory became the main candidate to describes our universe, it provides therefore a frame to study the history of it from 10^{-2} s to our present age, around 13.7 Gyr. However, this cosmological model yields various shortcomings. Two of the most relevant are the flatness and the horizon problems.

It was realized by Guth that a period of very rapid expansion at early times (that happened between $10^{-34\pm 6}$ s and $10^{-32\pm 6}$ s [2]), called inflationary universe, solved the flaws of the SBB theory [3]. Indeed, inflation predicts a flat universe where all relevant scales were casually connected, thus the SBB framework takes place not having these issues. The inflationary paradigm is mainly characterised by the existence of an homogeneous scalar field, the inflaton ϕ , which is the cause of an abrupt exponential expansion; and from a specific inflaton potential yields distinct scenarios. Also, the presumed presence of quantum fluctuations $\delta\phi$ around ϕ . It is this last feature that provides a clever mechanism to generate a primordial spectrum of density perturbations [4] (or primordial power spectrum) almost scale invariant (a power-law) and nearly Gaussian, which might explain the anisotropies of the CMB temperature map, hence generating the seeds for large scale structure in the universe.

In the standard inflationary picture, called cold inflation (CI), the super fast period of accelerated expansion quickly dilutes away all traces of any pre-inflationary matter or radiation density, leaving this framework in a vacuum state. However, this yields a supercooled universe. So in order to successfully explain the transition from inflation to the

*Electronic address: crojas@yachaytech.edu.ec

†Electronic address: rafaelhernandezjnz@gmail.com

SBB scenario, and hence the physics of recombination leading to the CMB that we observe today, the inflaton energy density necessarily requires to be transferred into ordinary matter and radiation, and thus to its interactions with other fields. Accordingly, the inflaton field could be coupled to other components and might dissipate its vacuum energy and warm up the universe. This alternative scenario is known as the warm inflation (WI) paradigm [5–8], where dissipative effects and associated particle production can, in fact, sustain a thermal bath concurrently with the accelerated expansion of the universe during inflation. Hence, this augmented mechanism becomes phenomenological more relevant. Certainly, WI has attractive characteristics. For instance, even if radiation is subdominant during inflation, it may smoothly become the leading component at the end of inflation, with no need for a separate reheating or preheating period. Moreover, dissipation also affects scalar perturbations, albeit for WI the fluctuations of the inflaton are thermally induced, which are already classical upon definition, hence they may bring an interpretation of the nature of the classical inhomogeneities observed in the CMB; consequently, there is no need to explain the troublesome quantum-to-classical transition problem of CI, due to the purely quantum origin of the CI density perturbations. Importantly, it has been observed that many scenarios of WI are within the observable window [9–11]. Moreover, it is been shown that WI can dodge the proposed swampland conjectures [11–13]. Thus, WI is in accordance with both the current cosmological observations and the proposed Swampland Criteria.

On the other hand, the Planck 2018 results favor inflation [14]. Indeed, the data is consistent with a flat universe, almost scale invariant, and nearly Gaussian primordial power spectrum. Different inflation models lead to distinct predictions; however, one has to be able to discriminate among existing templates using the recent CMB data, and, in addition to determine the shape of the primordial power spectrum. Although, the Planck 2018 results do not provide statistically significant evidence for features in the angular power spectrum [14], this possibility is explored, and has been widely discussed, first by Starobinsky [15], and later for a several number of authors [16–25]. These features could be caused by a step in the inflationary potential which lead to oscillations in the scalar power spectrum. Adams [16] has proposed a particular model where a step feature is added to the chaotic inflationary potential, $V_0 = m^2 \phi^2/2$, in the following way (see fig. 1):

$$V(\phi) = \frac{1}{2} m^2 \phi^2 \left[1 + c \tanh \left(\frac{\phi - \phi_{\text{step}}}{d} \right) \right], \quad (1)$$

where the step occurs at $\phi = \phi_{\text{step}}$, m is the inflaton mass, and the parameters c and d are related to the amplitude and width of the feature, respectively. The presence of the step does not interrupt inflation but introduces oscillations in the primordial power spectrum that depend on the height and gradient of the step, and as a consequence it will be scale dependent.

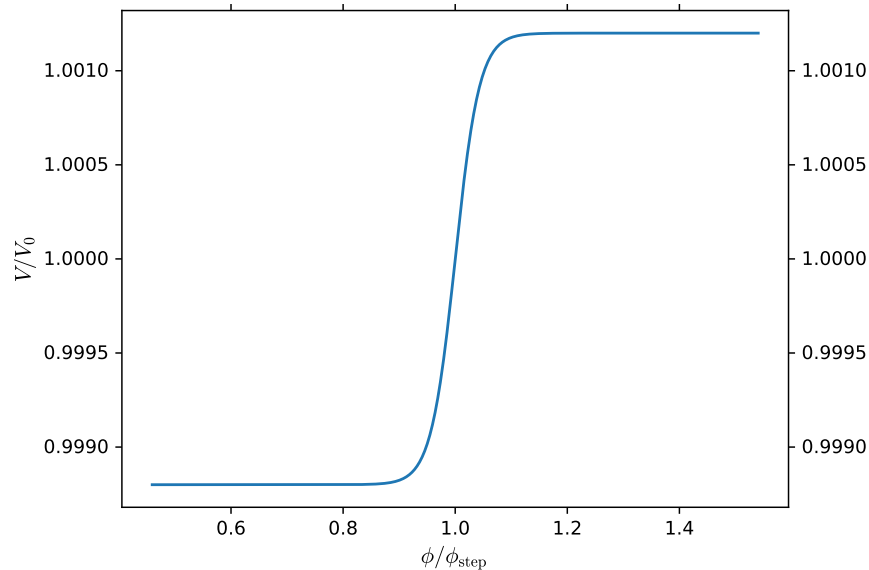


FIG. 1: The evolution of V/V_0 as a function of the normalised inflaton field ϕ/ϕ_{step} . We take $m = 5.731 \times 10^{-6} M_{Pl}$, $\phi_{\text{step}} = 15.451 M_{Pl}$, $c = 0.0012$, $d = 0.04 M_{Pl}$, and the initial value of the inflaton $\phi_0 = 16.706 M_{Pl}$. Note that the step occurs at $\phi/\phi_{\text{step}} \simeq 1$.

In this work we present an analysis of an inflationary framework of a chaotic potential with a step from the CI and WI perspectives. We solve numerically all background and linear-perturbed variables, which in turn will allow to scan all relevant parameters along a large range of scales. We take a pivot wave number k_0 when the step occurs. On the one hand, we study thoroughly the CI case where we find outcome regions within the observational window. On the other hand, the WI instance is presented, therein we show main differences between the CI and WI scenarios.

This paper is organized as follows. On the one hand, in section II we exhaustively study a CI scenario. On the other hand, in section III we describe a WI case; and we briefly contrast main differences between these frameworks. Finally, in section IV we will give the conclusion and outlook of this work.

II. SINGLE FIELD INFLATION: COLD INFLATION

We start with a model described by the nonzero vacuum expectation value of the inflaton field $\phi(t)$ on the homogeneous and isotropic state, this carries most of the energy of the universe, hence any other matter content must be subdominant. Additionally, its fluctuation $\delta\phi(\mathbf{x}, t)$, which describes the quantum fluctuation around ϕ . We will work within a homogeneous and isotropic flat Friedmann-Lemaître-Robertson-Walker (FLRW) metric:

$$ds^2 = -dt^2 + a(t)^2 \delta_{ij} dx^i dx^j, \quad (2)$$

where t is the cosmological time, $a = a(t)$ is the scale factor. Then in the cosmological case the universe inflates as the field is rolling down the hill. The dynamic equations are

$$H^2 = \frac{\rho_\phi}{3M_{Pl}^2}, \quad (3)$$

$$\ddot{\phi} + 3H\dot{\phi} + V_\phi = 0, \quad (4)$$

where $\rho_\phi = \dot{\phi}^2/2 + V(\phi)$ is the energy density of the inflaton, V_ϕ is the derivative of the potential energy with respect to the field and $H = \dot{a}/a$ is the expansion rate or Hubble parameter. Also $M_{Pl} = 1/\sqrt{8\pi G}$ is the reduced Planck mass. The first expression is called Friedmann constraint, the second one is the scalar field equation Klein-Gordon or the energy-momentum conservation equation. As we mentioned before, inflation requires for instance that $\rho_r(\text{radiation}) \ll \rho_\phi$ in order to generate the abrupt expansion; however, any other present subdominant component might play an important role at the end of inflation. Indeed, this is the study case for the next section in this paper. The amount by which the universe inflates is measured as the number of e-foldings N_e , and since the size of the expansion is expected to be an enormous quantity, it is useful to compute it in terms of the logarithm of the ratio of the scale factor between the end of inflation and a time t during inflation defined by:

$$N_e \equiv \ln \left[\frac{a(t_{end})}{a(t)} \right] = \int_t^{t_{end}} dt H. \quad (5)$$

Typically between 40 and 60 e-foldings of observable inflation^a are large enough to solve the horizon and flatness problems. Finally, inflation last while the slow-roll parameter $\epsilon_H = -\dot{H}/H^2 < 1$, where $\dot{H} = -\dot{\phi}^2/2/M_{Pl}^2$, so it ends when $\epsilon_H = 1$. Moreover, an inflationary scenario also requires a flat potential. This condition is measured by the $\eta_H = -\ddot{\phi}/(H\dot{\phi})$ parameter. Where a particular potential preserves flatness having $|\eta_H| < 1$. For the time being, above system, Eqs. (3,4), represents only the background dynamics. However, we must introduce the fluctuations of such physical system. First, we present the spacetime metric for a scalar-type of perturbation in the *zero-shear gauge* is given by [26]:

$$ds^2 = -(1 + 2\alpha)dt^2 + a^2 [\delta_{ij}(1 - 2\alpha)] dx^i dx^j, \quad (6)$$

where α is spacetime-dependent perturbed-order variable. Then, for the inflaton we replace the scalar field by $\phi + \delta\phi$, and using the perturbed metric Eq. (6) to get the first order perturbation equations [27, 28]:

$$\delta\ddot{\phi} + 3H\delta\dot{\phi} + \left(\frac{k^2}{a^2} + V_{\phi\phi} \right) \delta\phi = 4\dot{\alpha}\dot{\phi} + (2\ddot{\phi} + 6H\dot{\phi})\alpha, \quad (7)$$

$$\ddot{\alpha} + 4H\dot{\alpha} + (3H^2 + 2\dot{H})\alpha = \frac{\dot{\phi}\delta\dot{\phi} - \dot{\phi}^2\alpha - V_\phi\delta\phi}{2M_{Pl}^2}. \quad (8)$$

^a CMB fluctuations, from the size of the observable universe down to the size of galaxies, were generated during ~ 10 e-folds about 60 e-folds before the end of inflation.

We will evolve the equations for the perturbations at linear order, for a given model, without approximations and working in the *zero-shear gauge*. For a scalar field, the power spectrum of the comoving curvature perturbation \mathcal{R} is:

$$P_{\mathcal{R}} = \frac{k^3}{2\pi^2} \left(\frac{H}{\dot{\phi}} \right)^2 |\delta\phi^{GI}|^2, \quad \text{where} \quad \delta\phi^{GI} = \delta\phi + \frac{\dot{\phi}}{H} \alpha. \quad (9)$$

In order to contrast the observable parameters with Planck data, we need to evaluate, at horizon crossing, the scalar spectral index n_s and the tensor-to-scalar ratio r which are defined as

$$n_s - 1 \equiv \frac{d \ln P_{\mathcal{R}}}{d \ln k}, \quad r = \frac{P_h}{P_{\mathcal{R}}}, \quad (10)$$

where P_h is the tensor power spectrum^b. However, numerically we evaluate n_s and r when $P_{\mathcal{R}}$ and P_h become constant, approximately two times after horizon crossing.

A. CI results:

To study the effects of features on the spectrum of primordial perturbations we consider the following numerical example. We take $m = 5.731 \times 10^{-6} M_{Pl}$, $\phi_{\text{step}} = 15.451 M_{Pl}$, $c = 0.0012$, $d = 0.04 M_{Pl}$, and the initial value of the inflaton $\phi_0 = 16.706 M_{Pl}$. Inflation lasts $N_e = 70.2$, and the step occurs at $\phi = \phi_{\text{step}}$ around $N_e \simeq 10.1$. Therefore, from the time of the step about 60 e-folds of inflation take place.

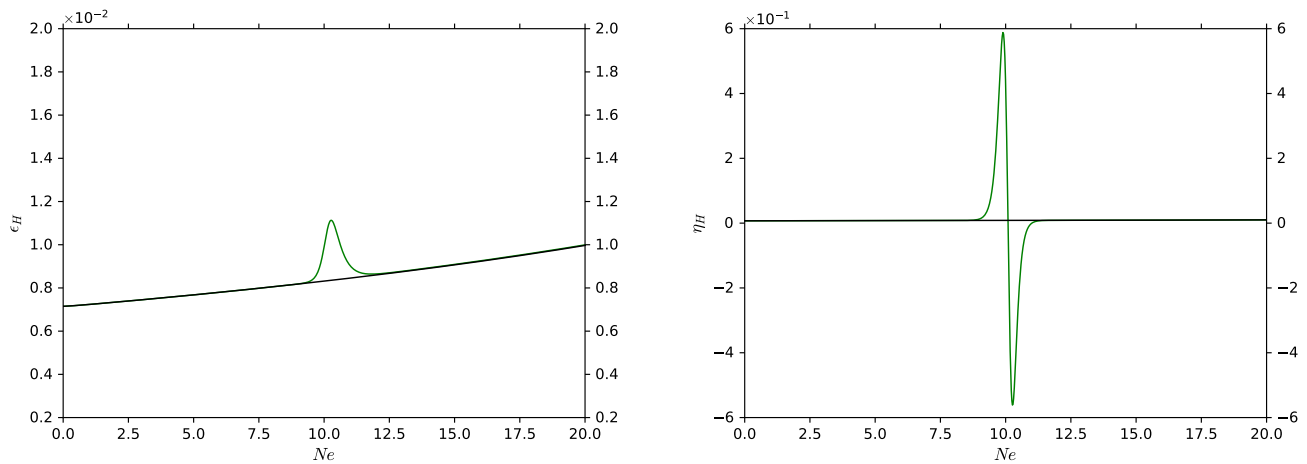


FIG. 2: Behaviour of the slow-roll parameters ϵ_H and η_H with respect to the number of e-folds N_e within the CI scheme, described by a step (green) and a quadratic chaotic (black) potentials for 70.2 e-folds of inflation. Note that the step occurs at $N_e \simeq 10$.

In fig. 2 we show the effects of the features on the slow-roll parameters with respect to the number of e-foldings N_e . The black line characterises a quadratic chaotic description, whilst the green one corresponds to a step potential. Indeed, the feature occurs around $N_e \simeq 10$, from there both schemes evolve equally. This upshot will be determined when analysing the linear perturbations.

Prior to continue our analysis, we must explicitly explain how to compute the pivot scale k_0 . Since we solve numerically all variables, we estimate the feature of the potential when $\phi/\phi_{\text{step}} \simeq 1$ at a particular $N_e(\text{step})$, from there we equate $k_0 = a(N_e(\text{step}))H(N_e(\text{step}))$. Thus, we set up our reference value k_0 when the step occurs.

Then, fig. 3 shows the behaviour of the square root of the curvature power spectra $P_{\mathcal{R}}^{1/2}$ with respect to N_e . We only present the outcome of two distinct scales $k/k_0 \simeq 1, 4.4 \times 10^{-3}$, where $k_0 \simeq 0.0256 h \text{ Mpc}^{-1}$. This figures helps us to illustrate how the step spectrum behaves comparing with the featureless one. Actually, many of our results are

^b Tensor perturbations are described by: $\ddot{h}_k + 3H\dot{h}_k + \frac{k^2}{a^2}h_k = 0$. And the the tensor power spectrum is $P_h = \frac{4k^3}{\pi^2} |h_k|^2$.

very similar to [16–25], and in particular to [25]. Moreover, note that even the solid lined case, when horizon crossing $N_e^* \simeq 4.64$, $P_{\mathcal{R}}^{1/2}$ abruptly changes when the step occurs, which might indicate that this particular perturbation is not longer “freeze in” on super-horizon scales; however, after a short period this featured comoving curvature fluctuation becomes in fact constant, therefore its horizon re-entry value is different from the horizon exit one. This outcome might suggest that purely adiabatic primordial density perturbations no longer holds at the time of the step. Nonetheless, a deeper study is needed to assure that entropy production is indeed happening at super-horizon scales.

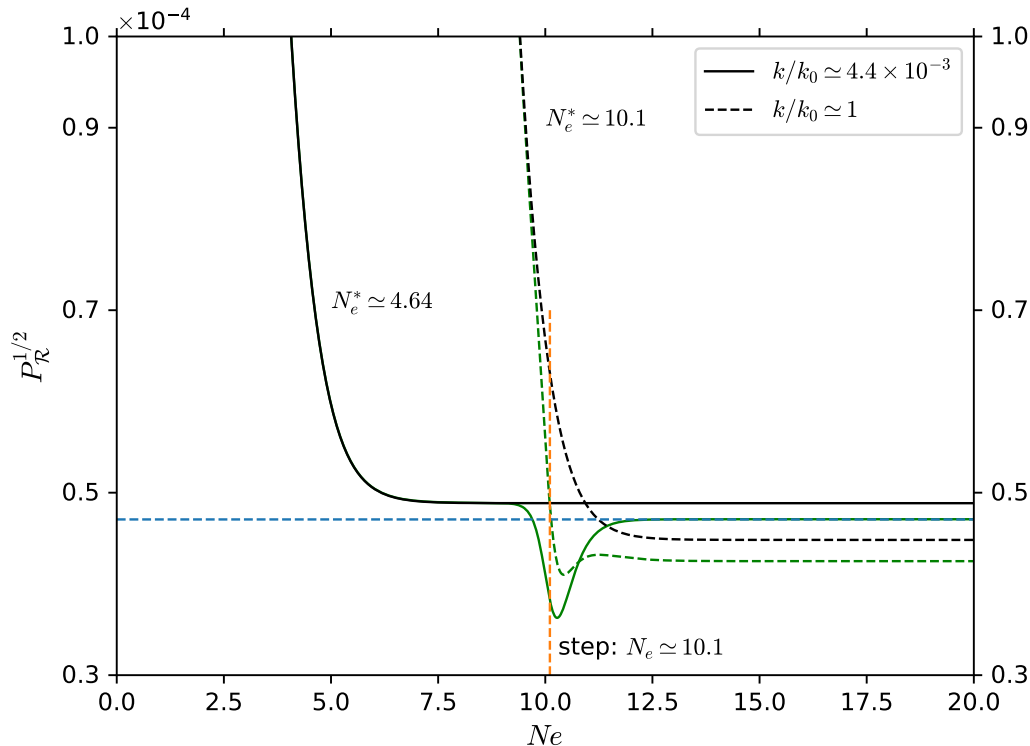


FIG. 3: Behaviour of the square root of the curvature power spectra $P_{\mathcal{R}}^{1/2}$ with respect to the number of e-folds N_e , described by a step (green) and a quadratic chaotic (black) potentials for 70.2 e-folds of inflation. We show the outcome for two different wave numbers $k/k_0 \simeq 1, 4.4 \times 10^{-3}$, where $k_0 \simeq 0.0256 h \text{Mpc}^{-1}$. Solid lines correspond to $N_e^* \simeq 4.64$, whilst dashed lines are at $N_e^* \simeq 10.1$. The blue dashed line corresponds to the CMB observations by Planck Legacy value $P_{\mathcal{R}}^{1/2} \simeq 4.7 \times 10^{-5}$ [29].

In the next examples we change a bit the initial parameters, since we set $P_{\mathcal{R}} \simeq 2.22 \times 10^{-9}$ [29] at $k_0 \simeq 0.04 h \text{Mpc}^{-1}$. Then, to normalise $P_{\mathcal{R}}$ with respect to above value we take $m = 6.3 \times 10^{-6} M_{Pl}$, $\phi_{\text{step}} = 15.5 M_{Pl}$, $c = 0.0012$, $d = 0.04 M_{Pl}$, and the initial value of the inflaton $\phi_0 = 16.8 M_{Pl}$. Now, inflation lasts $N_e = 71.0$, but the step occurs at $\phi = \phi_{\text{step}}$ around $N_e \simeq 10.5$. Therefore, once again, from the time of the step about 60 e-folds of inflation take place. The following plots figs. 4, 5, 6, and 7 will show all relevant observable parameters. We perform a wide scan of the scale k in terms of a pivot wave number k_0 , and we numerically evaluate all quantities two times after horizon crossing, since we check that indeed $P_{\mathcal{R}}$ and P_h become constant at this point in time.

Let us examine fig. 4. First, the upshot of the power spectrum is in good agreement with the results of Cadavid [25], where his conclusions indicates that a step in the potential can cause significant changes to the spectrum at scales around k_0 . Additionally, we include the evolution of a featureless instance, in order to exemplify how the oscillatory proposal distances from the chaotic potential for approximately two decades $0.2 < k/k_0 < 20$; however, both $P_{\mathcal{R}}$ behave the same before and after this range. On the other hand, figs. 5, 6, and 7 bring new aspects of this model. We plot the evolution of the scalar spectral index n_s with respect to k ; n_s versus the tensor to scalar ratio r ; and r versus k . As expected a quadratic chaotic scenario presents a nearly scale invariant n_s ^c, whilst the potential with

^c In order to compute the scalar spectral index n_s , we implement a numerical code to compute the numerical derivative $n_s - 1 \equiv \frac{d \ln P_{\mathcal{R}}}{d \ln k}$.

a step yields an oscillatory n_s ; where it fluctuates from negative values to bigger than one. This outcome certainly needs further analysis, and it is left for a future work. In addition, more than one region of (n_s, r) , see fig. 6, was brought back to the observation window. And in particular, from fig. 7 one can compute the minimum of $r \simeq 0.084$ that corresponds to $k/k_0 \simeq 2.43$; where this value indeed lies within the observable contours [29, 33].

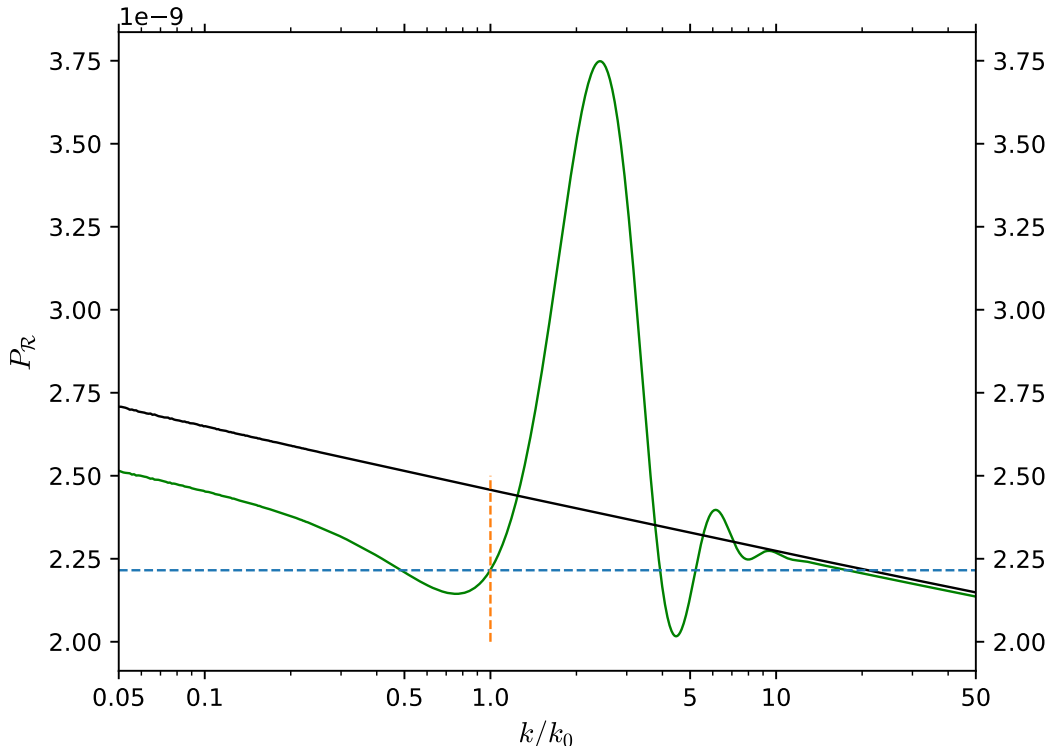


FIG. 4: Behaviour of the curvature power spectra $P_{\mathcal{R}}$ with respect to the ratio k/k_0 , where $k_0 \simeq 0.04 h \text{ Mpc}^{-1}$, described by a step (green) and a quadratic chaotic (black) potentials for 71.0 e-folds of inflation. The orange vertical line corresponds to $k/k_0 = 1$ and $P_{\mathcal{R}} \simeq 2.22 \times 10^{-9}$. On the other hand, the blue dashed line corresponds to the CMB observations by Planck Legacy value $P_{\mathcal{R}} \simeq 2.22 \times 10^{-9}$ [29].

Notwithstanding, we analysed in great detail a CI model, in the next section we will present an enhanced scenario: WI.

III. WARM INFLATION

To begin with, WI brings radiation into the evolution of inflation. Thus, a thermal bath imbibes the inflaton field, modifying the dynamics both at the background and the perturbation level. At first the main input is to introduce a dissipative term $\Upsilon \dot{\phi}$ in the inflaton evolution equation, as a source of radiation production [5–8]. To be able to describe this mechanism, all macroscopic motion must be slow relative to the relevant microscopic time scales, then the macroscopic dynamics can be treated adiabatically. To ensure the aforementioned near-equilibrium process, one must satisfy the adiabatic condition, namely $\Gamma/H > 1$, where Γ is the decay width, which quantifies the microscopic interactions; and H corresponds to a macroscopic measurement. Posteriorly, a noise force term was included to also drive the inflaton fluctuations, with a fluctuation-dissipation theorem uniquely specifying the inflaton fluctuations

We use Python [30]: `numpy.diff` [31]; and `scipy.interpolate` [32].

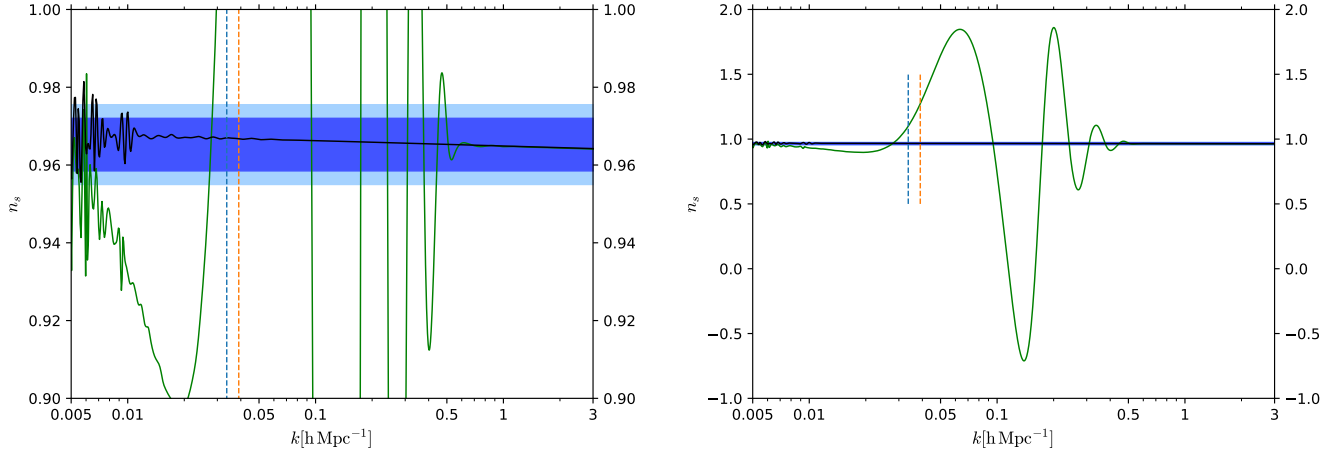


FIG. 5: Evolution of the scalar spectral index n_s with respect to k , described by a step (green) and a quadratic chaotic (black) potentials for 71.0 e-folds of inflation. The orange vertical line corresponds to $k_0 \simeq 0.04 h \text{ Mpc}^{-1}$. On the other hand, the blue dashed line corresponds to the CMB observation by Planck Legacy pivot value $k_* \simeq 0.0336 h \text{ Mpc}^{-1}$ ($k_* \simeq 0.05 \text{ Mpc}^{-1}$) [29, 33]. The blue contours correspond to the 68% and 95% C.L. results from Planck 2018 TT,TE,EE+lowE+lensing data [29, 33].

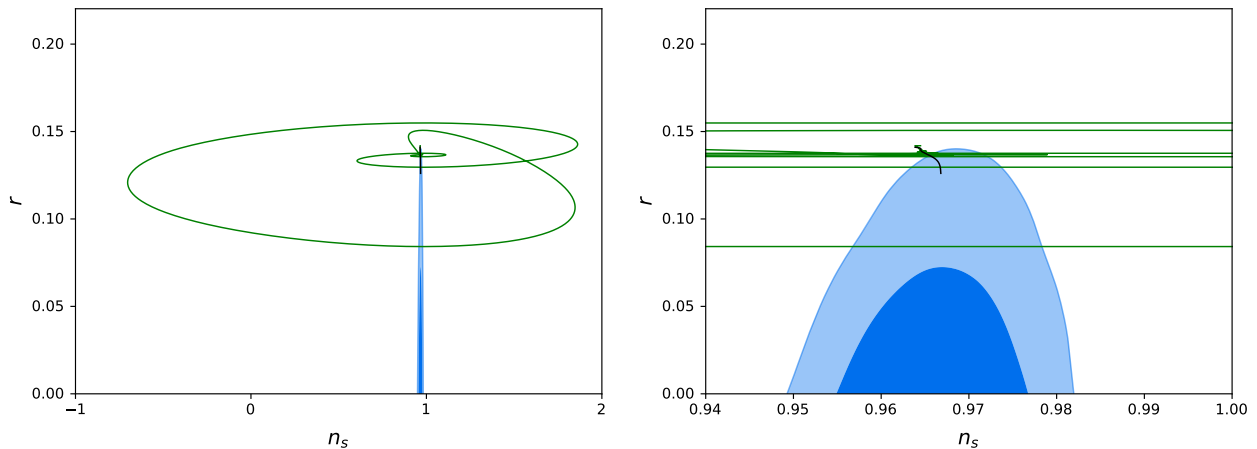


FIG. 6: Observable parameters: scalar spectral index n_s and the tensor to scalar ratio r . This plot shows the allowed trajectories in the (n_s, r) plane, described by a step (green) and a quadratic chaotic (black) potentials for 71.0 e-folds of inflation. The blue contours correspond to the 68% and 95% C.L. results from Planck 2018 TT,TE,EE+lowE+lensing data [29, 33].

[5–8]. Thus, we will start with the WI background evolution equations for the inflaton-radiation system, given by:

$$\begin{aligned} \ddot{\phi} + (3H + \Upsilon)\dot{\phi} + V_\phi &= 0, \\ \dot{\rho}_r + 4H\rho_r &= \Upsilon\dot{\phi}^2, \end{aligned} \quad (11)$$

where $\Upsilon = \Upsilon(T, \phi)$ is the dissipative coefficient^d in the leading adiabatic approximation, and it is computed from first principles provided the relevant interactions between the scalar field and the thermalised degrees of freedom (dof); $\rho_r = \pi^2 g_* T^4/30$, g_* being the effective no. of light dof. And once again dots correspond to time derivatives, V_ϕ is the derivative of the potential energy with respect to the field, and H is the Hubble parameter, given by the Friedmann

^d Indeed, Υ can depend on either temperature T or ϕ or both. For instance, a particular supersymmetric model yields a dissipative coefficient $\Upsilon \propto T^3/\phi^2$ [34].

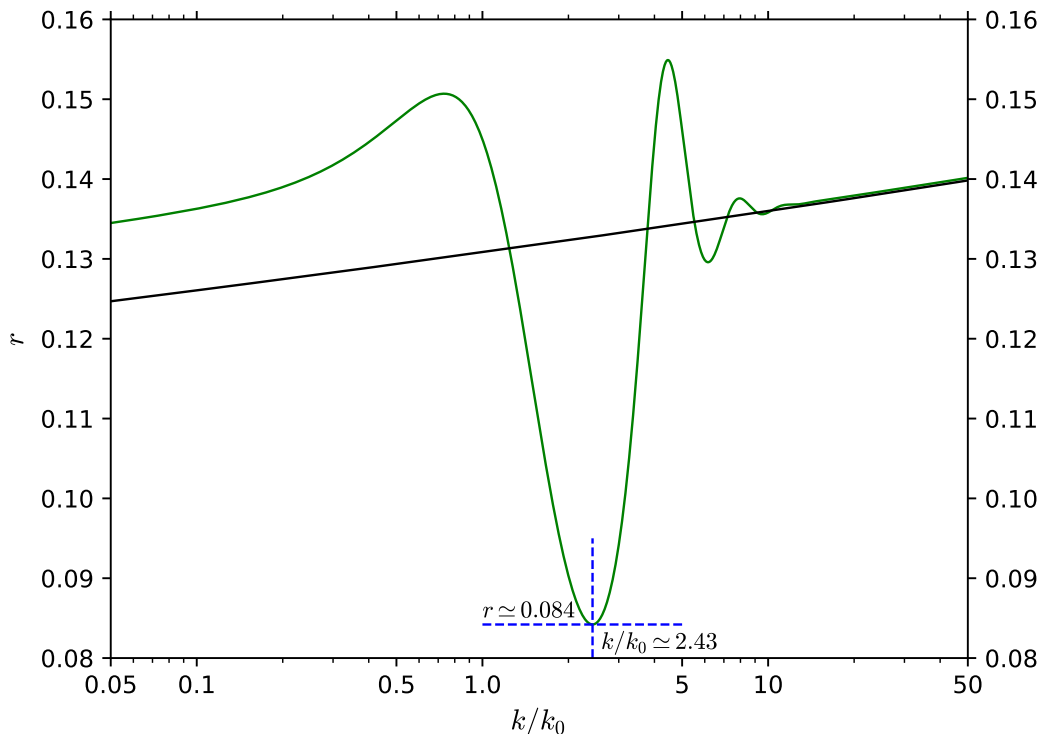


FIG. 7: Behaviour of the tensor to scalar ratio r with respect to k/k_0 , where $k_0 \simeq 0.04 h \text{ Mpc}^{-1}$, described by a step (green) and a quadratic chaotic (black) potentials for 71.0 e-folds of inflation. Note that the minimum value $r \simeq 0.084$ corresponds to $k/k_0 \simeq 2.43$. Indeed, this outcome lies within the Planck contours [29].

equation for a flat FRW universe:

$$3H^2 = \frac{\rho}{M_{Pl}^2}, \quad (12)$$

where $\rho = \rho_\phi + \rho_r$ is the total energy density, with $\rho_\phi = \dot{\phi}^2/2 + V(\phi)$. Also the field pressure and the equation of state for the radiation degrees of freedom are $p_\phi = \dot{\phi}^2/2 - V(\phi)$ and $p_r = \rho_r/3$ respectively. The dissipation coefficient is given by [11]:

$$\Upsilon = C_\phi \phi^n, \quad n \geq 1, \quad (13)$$

where this expression comes from the dynamics of a supersymmetric distributed mass (DM) model. This particular scheme arises from a general form of an effective $N = 1$ global SUSY theory version of the DM model with chiral superfields Φ , X_i and Y_i [34–37]. The chiral superfields Φ , X_i and Y_i have (scalar, fermion) components (ϕ, ψ_ϕ) , (χ_i, ψ_{χ_i}) and $(\sigma_i, \psi_{\sigma_i})$, respectively. Thus, $g_* = 1 + 15N_M/4$, N_M being the no. of bosonic χ_i (fermionic ψ_i) light degrees of freedom at horizon crossing. There are more consistent with microscopic derivations of a the temperature independent Υ (see, e.g., refs.[38–42]). In addition, in the DM model, the average decay width $\Gamma \propto T$ [11]. During inflation the motion of the inflaton field has to be overdamped in order to end the accelerated expansion, and indeed this can be achieved due to either the Hubble rate, as the CI case, or an extra friction Υ term, or the interaction of both components. We can quantify this competition by defining the dissipative ratio $Q = \Upsilon/(3H)$. According to the ratio Q we will have distinct cases: for $Q < 1$, this is called weak dissipative warm inflation (WDWI); and when $Q \geq 1$ we are in strong dissipative warm inflation (SDWI). Importantly, given the presence of radiation during inflation, the potential acquires thermal corrections, and indeed they become relevant at the background and fluctuation levels, since they adjust the slow-roll parameter ϵ_H . However, in the scenario with a quartic chaotic potential $V(\phi) = \lambda\phi^4/4$ within the SDWI, such thermal corrections give a negligible contribution to both the effective potential and its first derivative in the perturbative regime [11]. And we expect a similar outcome with a chaotic potential inflationary

potential $V(\phi) = m^2\phi^2/2$, within the SDWI. Hence, we will not consider these thermal corrections. Moreover, in order to describe a near-equilibrium process, one must satisfy thermalisation, that is the adiabatic condition $\Gamma/H > 1$, which translates roughly into $T/H > 1$ since $\Gamma \propto T$ [11].

Once again we have to introduce the scalar perturbations; however, for WI these are also accompanied by thermal fluctuations. Hence, during WI we have a multicomponent fluid: a mixture of a scalar field (the inflaton) interacting with the radiation fluid. The equations for the perturbations in a multicomponent fluid can be found for example in [26, 28, 43]. Working in momentum space, defining the Fourier transform with respect to the comoving coordinates, the equation of motion for the radiation and momentum fluctuations with comoving wavenumber k are given by [26]:

$$\delta\dot{\rho}_r + 4H\delta\rho_r = 4\rho_r\dot{\alpha} + \frac{k^2}{a^2}\Psi_r + \delta Q_r + Q_r\alpha, \quad (14)$$

$$\dot{\Psi}_r + 3H\Psi_r = -\frac{\delta\rho_r}{3} - \frac{4\rho_r}{3}\alpha - \Upsilon\dot{\phi}\delta\phi, \quad (15)$$

where $Q_r = \Upsilon\dot{\phi}^2$, and $\delta Q_r = \delta\Upsilon\dot{\phi}^2 + 2\Upsilon\dot{\phi}\delta\dot{\phi} - 2\alpha\Upsilon\dot{\phi}^2$. We have also used the equation of state for the radiation degrees of freedom $\delta p_r = \delta\rho_r/3$. For a scalar field interacting with a fluid, the evolution equation for the field fluctuations $\delta\phi$, which is described by a stochastic evolution determined by the Langevin-like equation [5, 44–46]:

$$\delta\ddot{\phi} + (3H + \Upsilon)\delta\dot{\phi} + \left(\frac{k^2}{a^2} + V_{\phi\phi}\right)\delta\phi = (2(\Upsilon + H)T)^{1/2}a^{-3/2}\Xi_k - \delta\Upsilon\dot{\phi} + 4\dot{\alpha}\dot{\phi} + (2\ddot{\phi} + 6H\dot{\phi} + \Upsilon\dot{\phi})\alpha, \quad (16)$$

where $\Xi_k \equiv \Xi(\mathbf{k}, t)$ is a stochastic source that can be well approximated by a localised Gaussian distribution with correlation function given by:

$$\langle \Xi(\mathbf{k}, t)\Xi(\mathbf{k}', t') \rangle = \delta(t - t')\delta^{(3)}(\mathbf{k} - \mathbf{k}'). \quad (17)$$

And the evolution equation for the metric variable α is given by [26]:

$$\ddot{\alpha} + 4H\dot{\alpha} + (3H^2 + 2\dot{H})\alpha = \frac{1}{2M_{Pl}^2} \left(\dot{\phi}\delta\dot{\phi} - \dot{\phi}^2\alpha - V_{\phi}\delta\phi + \frac{\delta\rho_r}{3} \right). \quad (18)$$

Given that a particular gauge choice would depend on the problem at hand, hence in order to avoid any subsequent miscalculation, at linear order, following [26] we introduce the gauge invariant field, energy density and momentum perturbations:

$$\delta\phi^{GI} = \delta\phi + \frac{\dot{\phi}}{H}\alpha, \quad \Psi_{\phi}^{GI} = \Psi_{\phi} - \frac{\rho_{\phi} + p_{\phi}}{H}\alpha. \quad (19)$$

$$\delta\rho_r^{GI} = \delta\rho_r + \frac{\dot{\rho}_r}{H}\alpha, \quad \Psi_r^{GI} = \Psi_r - \frac{\rho_r + p_r}{H}\alpha, \quad (20)$$

with $\Psi_{\phi} = -\dot{\phi}\delta\phi$. For a multi-component fluid, the total gauge-invariant comoving curvature perturbation \mathcal{R} is given by:

$$\mathcal{R} = -\frac{H}{\rho + p}\Psi_T^{GI} = -\frac{H}{\rho + p}\sum_x \Psi_x^{GI} = \sum_x \frac{\rho_x + p_x}{\rho + p}\mathcal{R}_x, \quad (21)$$

where $\Psi_T^{GI} = \Psi_{\phi}^{GI} + \Psi_r^{GI}$, then $\rho = \rho_{\phi} + \rho_r$ is the total energy density, while $p = p_{\phi} + p_r$ is the total pressure, therefore $\rho + p = \dot{\phi}^2 + 4\rho_r/3$. Each fluid is labelled by a sub index “ x ”:

$$\mathcal{R}_x = -\frac{H}{\rho_x + p_x}\Psi_x^{GI}. \quad (22)$$

For instance, with a scalar field we have $\Psi_{\phi}^{GI} = -\dot{\phi}\delta\phi^{GI}$, yielding:

$$\mathcal{R}_{\phi} = \frac{H}{\dot{\phi}}\delta\phi^{GI} = \alpha + \frac{H}{\dot{\phi}}\delta\phi. \quad (23)$$

Since we work in a gauge-invariant domain, the primordial curvature perturbation has the property to be constant within few Hubble times after the horizon crossing ($k_* = a_*H_*$), therefore we can compute it at horizon exit and

remain ignorant about the subhorizon physics during and after reheating until horizon re-entry of a given \mathcal{R} -mode^e. The power spectrum of the comoving curvature perturbation \mathcal{R} is defined as:

$$P_{\mathcal{R}} = \frac{k^3}{2\pi^2} |\mathcal{R}|^2 = \frac{k^3}{2\pi^2} \left(\frac{H}{p + \rho} \right)^2 |\Psi_T^{GI}|^2. \quad (24)$$

As an example for a scalar field, the power spectrum of the comoving curvature perturbation \mathcal{R}_ϕ is given by:

$$P_{\mathcal{R}_\phi} = \frac{k^3}{2\pi^2} \left(\frac{H}{\dot{\phi}} \right)^2 |\delta\phi^{GI}|^2. \quad (25)$$

In the next subsection we will present an example of background and linear perturbations dynamics within a WI scenario.

A. WI results:

To study the effects of features on the spectrum of primordial perturbations we utilise a linear dissipative coefficient:

$$\Upsilon = C_\phi \dot{\phi}. \quad (26)$$

We consider above component, since there are certain favorable already published features. First, this example works properly without adding thermal contributions to the potential, provided the outcome comes from a SDWI [11], which is this case of study. Second, the adiabatic condition $\Gamma/H > 1$ or $T/H > 1$ is easily achieved in the SDWI; so there is no need to examine this thoroughly. Last but not the least, two swampland criteria, relevant for inflationary theories, have been intensively discussed [47, 48], $|\Delta\phi|/M_{Pl} < \Delta$ and $M_{Pl}|V_\phi|/V > c$, provided that $V > 0$, where $\{\Delta, c\} \sim \mathcal{O}(1)$. And these criteria are very consistent with a WI paradigm described by a DM model [11]. In fact, it was noted that inherently the dissipative feature in WI makes it amenable for consistency with swampland criteria, as already noted in the literature [12, 13, 49–51]. We take $m = 3.09897 \times 10^{-8} M_{Pl}$, $\phi_{step} = 0.778 M_{Pl}$, $c = 0.012$, $d = 0.04 M_{Pl}$, $C_\phi = 1.5 \times 10^{-5}$, and $N_M = 10$. Also the initial value of the inflaton $\phi_0 = 0.845 M_{Pl}$. Inflation lasts $N_e = 70.2$. The step occurs at $\phi = \phi_{step}$ around $N_e \simeq 10.1$. However, note that the parameter c is one order of magnitude bigger than one in CI case. We run a few examples with $c = 0.002$, yet the feature of potential was not noticeable. So we decided to increment c in order to show such distinctive characteristics of $V(\phi)$. In addition, given aforementioned set of input values, we guarantee the system is within a SDWI regime; and indeed, the parameter $Q_* \geq 390$.

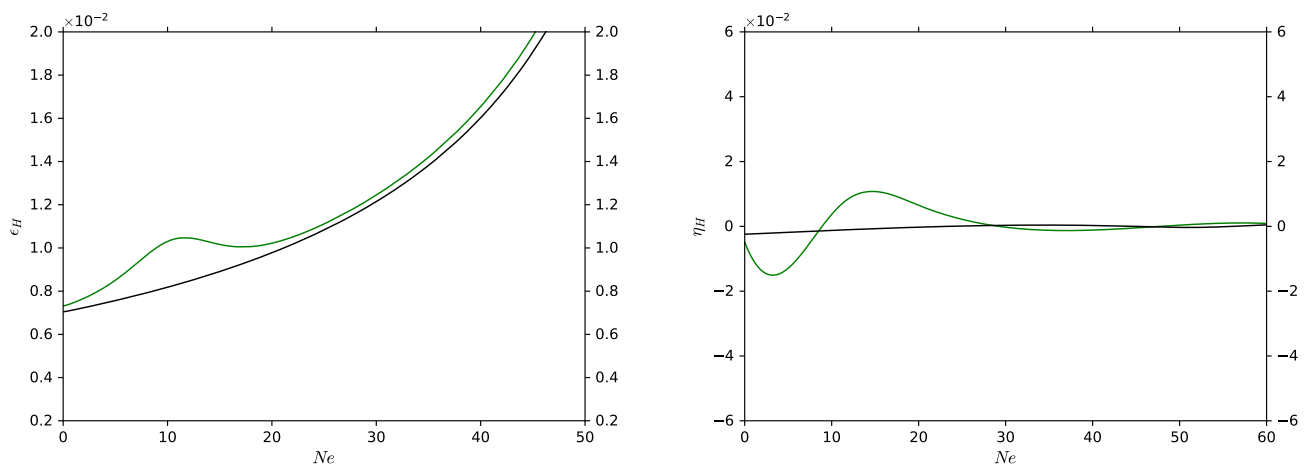


FIG. 8: Behaviour of the slow-roll parameters ϵ_H and η_H with respect to the number of e-folds N_e within the WI scheme, described by a step (green) and a quadratic chaotic (black) potentials for 70.2 e-folds of inflation. Note that the step occurs at $N_e \simeq 10$.

^e \mathcal{R} becomes constant on super-horizon scales; perturbations with comoving wave number k are said to “freeze in” as soon as the comoving Hubble horizon shrinks so far that $k^{-1} > (aH)^{-1}$.

In fig. 8 we show the effects of the features on the slow-roll parameters with respect to the number of e-foldings N_e . The black line characterises a quadratic chaotic description, whilst the green one corresponds to a step potential. Once again, the feature occurs around $N_e \simeq 10$. Contrary to the CI case, the contrast between both potentials become more evident for longer number of e-folds, in fact, note how the η_H parameter (right hand of fig. 8) oscillates more than the CI example. Actually, this outcome will be determinant when analysing the linear perturbations, since we will numerically evaluate $P_{\mathcal{R}}$ and P_h approximately now three times after horizon crossing, where they certainly become constant.

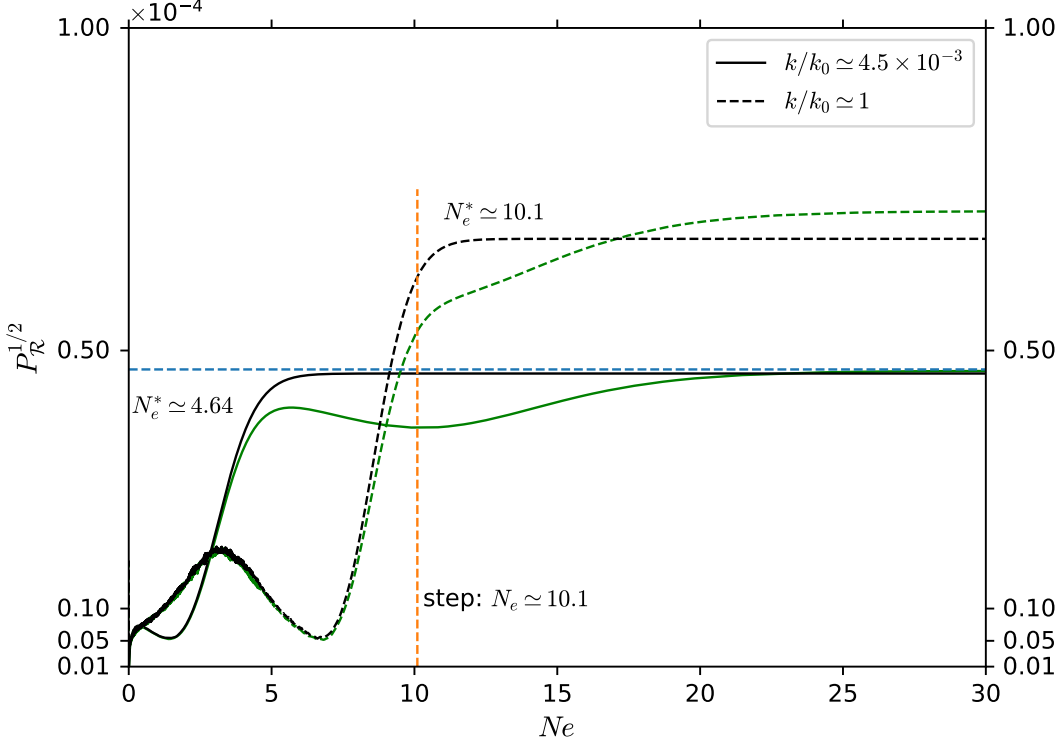


FIG. 9: Behaviour of the square root of the curvature power spectra $P_{\mathcal{R}}^{1/2}$ with respect to the number of e-folds N_e , described by a step (green) and a quadratic chaotic (black) potentials for 70.2 e-folds of inflation. We show the outcome for two different wave numbers $k/k_0 \simeq 1, 4.5 \times 10^{-3}$, where $k_0 \simeq 1.3 \times 10^{-3} h \text{Mpc}^{-1}$. Solid lines correspond to $N_e^* \simeq 4.64$, whilst dashed lines are at $N_e^* \simeq 10.1$. The blue dashed line corresponds to the CMB observations by Planck Legacy value $P_{\mathcal{R}}^{1/2} \simeq 4.7 \times 10^{-5}$ [29].

Then, fig. 9 shows the behaviour of the square root of the curvature power spectra $P_{\mathcal{R}}^{1/2}$ with respect to N_e . We only present the outcome of two distinct scales $k/k_0 \simeq 1, 4.5 \times 10^{-3}$, where $k_0 \simeq 1.3 \times 10^{-3} h \text{Mpc}^{-1}$. First, a straightforward result is the growth of the amplitude of the power spectrum before horizon crossing, this is due to the stochastic source $\Xi_k \equiv \Xi(\mathbf{k}, t)$. Then, this figures helps us to illustrate how the step spectrum behaves comparing with the featureless one. Note that in the solid lined example $P_{\mathcal{R}}^{1/2}$ changes smoothly when the step occurs, in contrast to CI. On the other hand, the second case $k/k_0 \simeq 1$ (dashed line), the step enhances the evolution of $P_{\mathcal{R}}^{1/2}$, where for a short period of time it slightly disconnects to the chaotic quadratic path, and in fact when both amplitudes become constant its gap value is larger than the $k/k_0 \sim 10^{-3}$. Which might indicate that for bigger scales this discrepancy would become more noticeable. Now both particular perturbations are not longer “freeze in” on super-horizon scales; however, after a short period this featured comoving curvature fluctuation becomes in fact constant, therefore its horizon re-entry values are definitely different from the horizon exit ones. Once again, this outcome might suggest that purely adiabatic primordial density perturbations no longer holds at the time of the step. Nonetheless, a deeper study is needed to assure that entropy production is indeed happening at super-horizon scales.

Moreover, we conjecture that WI could function as a screening mechanism capable of smoothing the feature of the inflationary potential, since at $k/k_0 \sim 1$ the step is reduced comparing to $k/k_0 \sim 10^{-3}$, then we expect this effect becomes even more evident at larger k/k_0 . Nonetheless, more work is needed to actually confirm this sentence.

Finally, one key aspect of this research was to contrast the features of an inflationary potential between both cold

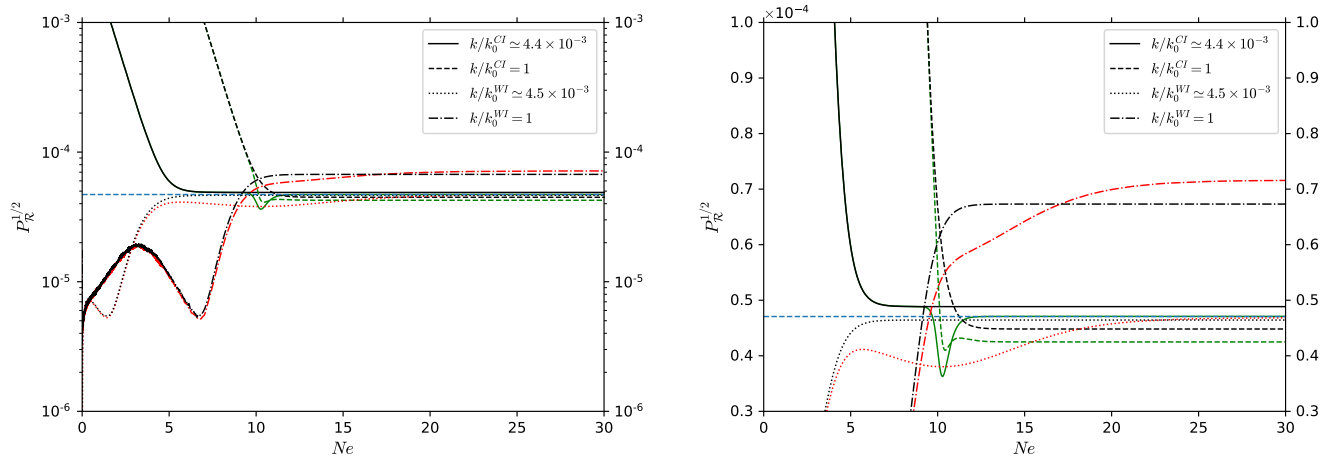


FIG. 10: Both cold and warm inflation comparative behaviour of the square root of the curvature power spectra $P_{\mathcal{R}}^{1/2}$ with respect to the number of e-folds N_e , described by a step (green and red) and a quadratic chaotic (black) potentials for 70 e-folds of inflation. We show the outcome for two different wave numbers $k/k_0 \simeq 1, 4 \times 10^{-3}$, and for both cold (green) and warm (red) inflation. Solid and dotted lines correspond to $N_e^* \simeq 4.6$, whilst dashed and dash-dot lines are at $N_e^* \simeq 10$. The blue dashed line corresponds to the CMB observations by Planck Legacy value $P_{\mathcal{R}}^{1/2} \simeq 4.7 \times 10^{-5}$ [29].

and warm scenarios. Hence, fig. 10 does show similarities and differences among various examples. At the same time, CI and WI exhibit an unequivocal step close to $\phi/\phi_{step} \simeq 1$ ($N_e \simeq 10$), and several e-folds after $P_{\mathcal{R}}$ becomes constant. However, a major distinction between both cases is the evident growth from $k/k_0 \sim 10^{-3}$ to $k/k_0 \sim 1$, although preliminary, of the warm $P_{\mathcal{R}}^{1/2}$ (red lines), opposite to CI instance (green lines). This upshot might suggest that the amplitude of the primordial spectrum can be much larger than the CMB value $P_{\mathcal{R}} \simeq 2.22 \times 10^{-9}$ [29] at large scales.

IV. FINAL REMARKS

The main purpose of this paper was to analyse thoroughly how an inflationary scenario from a chaotic potential with a step affects the relevant observational parameters. We work from two fronts: CI and WI.

In general terms, in the CI case the step indeed produces oscillations in the primordial power spectrum particularly around k_0 (see fig. 4), which belongs to the large scale perturbation sector. Then $P_{\mathcal{R}}$ evolves equally for both chaotic and step potentials. Even though many of our results are very similar to [16–25], and in particular to [25]; we have included the analysis of n_s and r . Indeed, we found that more than one region of (n_s, r) lies within the observable contours [29, 33]. And in particular, from fig. 7 one can compute the minimum of $r \simeq 0.084$ that corresponds to $k/k_0 \simeq 2.43$.

On the other hand, in the WI scenario, a straightforward result is the growth of the amplitude of the power spectrum before horizon crossing, this is due to the stochastic source $\Xi_k \equiv \Xi(\mathbf{k}, t)$. Also, the feature of the potential indeed induces perceptible changes in $P_{\mathcal{R}}$ around the step ($N_e \simeq 10$); however, these alterations become less evident for larger k/k_0 , which might indicate that for higher scales the effect of the step becomes less relevant. Moreover, one can observe that the step enhances the evolution of $P_{\mathcal{R}}^{1/2}$ when $k/k_0 \simeq 1$, where for a short period of time it slightly disconnects to the chaotic quadratic path, and in fact when both amplitudes become constant their gap values are larger than the $k/k_0 \sim 10^{-3}$ example. This might indicate that by increasing k/k_0 this discrepancy would become more noticeable. However, in order to asseverate previous sentences, we will study with much more details the WI case. Until then we are confident about our preliminary conclusions, since the two WI examples presented in this work provide us with reliable evidence to sustain our conjecture. Thus we envisage a complementary examination having a larger collection of data. Therefore, in a subsequent work we will scan a wide range of scales within a WI universe.

One remarkable upshot in both scenarios is that certain fluctuation scales are no longer “freeze in” on super-horizon scales. Thus, this outcome might suggest that purely adiabatic primordial density perturbations no longer holds at the time of the step. Nonetheless, a deeper study is needed to assure that entropy production is indeed happening at super-horizon scales.

Besides, a preliminary result is that $P_{\mathcal{R}}$ grows for larger fluctuation scales in WI. Contrary to the CI case. And recently WI has been proposed as a plausible mechanism that could lead to the formation of Primordial Black Holes on re-entry, provided the amplitude reaches a critical value $P_{\mathcal{R}} \sim 10^{-2}$ [52, 53]. And indeed, this opens new paths in which we can explore.

Acknowledgments

R.H.J is supported by CONACYT Estancias Posdoctorales por México, Modalidad 1: Estancia Posdoctoral Académica.

-
- [1] J. García-Bellido. Astrophysics and cosmology. <http://arxiv.org/abs/hep-ph/0004188>, 2000.
 - [2] A. R. Liddle and D. H. Lyth. *Cosmological inflation and large-scale structure*. Cambridge University Press, 2000.
 - [3] A. H. Guth. Inflationary universe: A possible solution to the horizon and flatness problems. *Phys. Rev. D*, 23:347, 1981.
 - [4] G. Chibisov and V. Mukhanov. Galaxy formation and phonons. *Mon. Not. R. Astron. Soc.*, 200:535, 1982.
 - [5] Arjun Berera and Li-Zhi Fang. Thermally induced density perturbations in the inflation era. *Phys. Rev. Lett.*, 74:1912–1915, 1995.
 - [6] Arjun Berera. Warm inflation. *Phys. Rev. Lett.*, 75:3218–3221, 1995.
 - [7] Arjun Berera. Interpolating the stage of exponential expansion in the early universe: A Possible alternative with no reheating. *Phys. Rev. D*, 55:3346–3357, 1997.
 - [8] Arjun Berera, Ian G. Moss, and Rudnei O. Ramos. Warm Inflation and its Microphysical Basis. *Rept. Prog. Phys.*, 72:026901, 2009.
 - [9] Mar Bastero-Gil, Arjun Berera, Rudnei O. Ramos, and Joao G. Rosa. Warm Little Inflation. *Phys. Rev. Lett.*, 117(15):151301, 2016.
 - [10] Mar Bastero-Gil, Arjun Berera, Rafael Hernández-Jiménez, and João G. Rosa. Dynamical and observational constraints on the Warm Little Inflation scenario. *Phys. Rev. D*, 98(8):083502, 2018.
 - [11] Mar Bastero-Gil, Arjun Berera, Rafael Hernández-Jiménez, and João G. Rosa. Warm inflation within a supersymmetric distributed mass model. *Phys. Rev. D*, 99(10):103520, 2019.
 - [12] Meysam Motaharfar, Vahid Kamali, and Rudnei O. Ramos. Warm inflation as a way out of the swampland. *Phys. Rev. D*, 99(6):063513, 2019.
 - [13] Suratna Das. Warm Inflation in the light of Swampland Criteria. *Phys. Rev. D*, 99(6):063514, 2019.
 - [14] Y. Akrami *et al.* Planck 2018 results. X. Constraints on inflation. *arXiv:1807.06211*, 2018.
 - [15] A. A. Starobinsky. Spectrum of adiabatic perturbations in the universe when there are singularities in the inflaton potential. *JETP Lett.*, 55:489, 1992.
 - [16] Adams, J. and Cresswell, B. and Easther, R. Inflationary perturbations from a potential with a step. *Phys. Rev. D*, 64:123514, 2001.
 - [17] P. Hunt and S. Sarkar. Multiple inflation and the WMAP “glitches”. *Phys. Rev. D*, 70:103518, 2004.
 - [18] L. Covi, J. Hamann, A. Melchiorri, A. Slosar and I. Sorbera. Inflation and WMAP three year data: features are still present. *Phys. Rev. D*, 74:083509, 2006.
 - [19] J. Hamann, L. Covi, A. Melchiorri, and A. Slosar. New constraints on oscillations in the primordial spectrum of inflationary perturbations. *Phys. Rev. D*, 76:023503, 2007.
 - [20] X. Chen, R. Easther, and E. A. Lim. Large non-Gaussianities in single-field inflation. *J. Cosmol. Astropart. Phys.*, 06:023, 2007.
 - [21] P. Hunt and S. Sarkar. Multiple inflation and the WMAP “glitches”. II. Data analysis and cosmological parameter extraction. *Phys. Rev. D*, 76:123504, 2007.
 - [22] J. Hamann, A. Shafieloo, and T. Souradeep. Features in the primordial power spectrum? A frequentist analysis. *J. Cosmol. Astropart. Phys.*, 04:010, 2010.
 - [23] N. Bartolo, D. Cannone, and S. Matarrese. The effective field theory of inflation models with sharp features. *J. Cosmol. Astropart. Phys.*, 10:038, 2013.
 - [24] A. G. Cadavid and A. E. Romano. Effects of discontinuities of the derivatives of the inflaton potential. *Eur. Phys. J. C*, 75:589, 2015.
 - [25] A. G. Cadavid. Features in single field slow-roll inflation. *J. Phys.: Conf. Ser.*, 831:012003, 2017.
 - [26] Jai-chan Hwang. Perturbations of the Robertson-Walker space - Multicomponent sources and generalized gravity. *Astrophys. J.*, 375:443–462, 1991.
 - [27] Jai-chan Hwang and Hyerim Noh. Cosmological perturbations with multiple fluids and fields. *Class. Quant. Grav.*, 19:527–550, 2002.
 - [28] Hideo Kodama and Misao Sasaki. Cosmological Perturbation Theory. *Prog. Theor. Phys. Suppl.*, 78:1–166, 1984.
 - [29] Y. Akrami *et al.* Planck 2018 results. I. Overview and the cosmological legacy of Planck. *arXiv:1807.06205*, 2018.
 - [30] Guido Van Rossum and Fred L. Drake. *Python 3 Reference Manual*. CreateSpace, Scotts Valley, CA, 2009.

- [31] Charles R. Harris, K. Jarrod Millman, Stéfan J. van der Walt, Ralf Gommers, Pauli Virtanen, David Cournapeau, Eric Wieser, Julian Taylor, Sebastian Berg, Nathaniel J. Smith, Robert Kern, Matti Picus, Stephan Hoyer, Marten H. van Kerkwijk, Matthew Brett, Allan Haldane, Jaime Fernández del Río, Mark Wiebe, Pearu Peterson, Pierre Gérard-Marchant, Kevin Sheppard, Tyler Reddy, Warren Weckesser, Hameer Abbasi, Christoph Gohlke, and Travis E. Oliphant. Array programming with NumPy. *Nature*, 585(7825):357–362, September 2020.
- [32] Pauli Virtanen, Ralf Gommers, Travis E. Oliphant, Matt Haberland, Tyler Reddy, David Cournapeau, Evgeni Burovski, Pearu Peterson, Warren Weckesser, Jonathan Bright, Stéfan J. van der Walt, Matthew Brett, Joshua Wilson, K. Jarrod Millman, Nikolay Mayorov, Andrew R. J. Nelson, Eric Jones, Robert Kern, Eric Larson, C J Carey, İlhan Polat, Yu Feng, Eric W. Moore, Jake VanderPlas, Denis Laxalde, Josef Perktold, Robert Cimrman, Ian Henriksen, E. A. Quintero, Charles R. Harris, Anne M. Archibald, António H. Ribeiro, Fabian Pedregosa, Paul van Mulbregt, and SciPy 1.0 Contributors. SciPy 1.0: Fundamental Algorithms for Scientific Computing in Python. *Nature Methods*, 17:261–272, 2020.
- [33] Y. Akrami et al. Planck 2018 results. X. Constraints on inflation. *Astron. Astrophys.*, 641:A10, 2020.
- [34] Mar Bastero-Gil and Arjun Berera. Warm inflation model building. *Int. J. Mod. Phys. A*, 24:2207–2240, 2009.
- [35] Lisa M H Hall and Ian G Moss. Thermal effects on pure and hybrid inflation. *Phys. Rev. D*, 71:023514, 2005.
- [36] Mar Bastero-Gil, Arjun Berera, and Rudnei O. Ramos. Dissipation coefficients from scalar and fermion quantum field interactions. *JCAP*, 09:033, 2011.
- [37] Mar Bastero-Gil, Arjun Berera, Rudnei O. Ramos, and Joao G. Rosa. General dissipation coefficient in low-temperature warm inflation. *JCAP*, 01:016, 2013.
- [38] H. P. de Oliveira and Rudnei O. Ramos. Dynamical system analysis for inflation with dissipation. *Phys. Rev. D*, 57:741–749, 1998.
- [39] Sergio del Campo, Ramon Herrera, and Diego Pavon. Cosmological perturbations in warm inflationary models with viscous pressure. *Phys. Rev. D*, 75:083518, 2007.
- [40] S. del Campo, R. Herrera, D. Pavón, and J. R. Villanueva. On the consistency of warm inflation in the presence of viscosity. *JCAP*, 08:002, 2010.
- [41] Rudnei O. Ramos. Fine tuning solution for hybrid inflation in dissipative chaotic dynamics. *Phys. Rev. D*, 64:123510, 2001.
- [42] Rudnei O. Ramos and L. A. da Silva. Power spectrum for inflation models with quantum and thermal noises. *JCAP*, 03:032, 2013.
- [43] Karim A. Malik, David Wands, and Carlo Ungarelli. Large scale curvature and entropy perturbations for multiple interacting fluids. *Phys. Rev. D*, 67:063516, 2003.
- [44] Arjun Berera. Warm inflation at arbitrary adiabaticity: A Model, an existence proof for inflationary dynamics in quantum field theory. *Nucl. Phys. B*, 585:666–714, 2000.
- [45] Lisa M. H. Hall, Ian G. Moss, and Arjun Berera. Scalar perturbation spectra from warm inflation. *Phys. Rev. D*, 69:083525, 2004.
- [46] E. Calzetta and B. L. Hu. Nonequilibrium Quantum Fields: Closed Time Path Effective Action, Wigner Function and Boltzmann Equation. *Phys. Rev. D*, 37:2878, 1988.
- [47] Georges Obied, Hiroshi Ooguri, Lev Spodyneiko, and Cumrun Vafa. De Sitter Space and the Swampland. *arXiv.*, 6 2018.
- [48] Prateek Agrawal, Georges Obied, Paul J. Steinhardt, and Cumrun Vafa. On the Cosmological Implications of the String Swampland. *Phys. Lett. B*, 784:271–276, 2018.
- [49] Suratna Das. Note on single-field inflation and the swampland criteria. *Phys. Rev. D*, 99(8):083510, 2019.
- [50] Zhu Yi and Yungui Gong. Gauss–Bonnet Inflation and the String Swampland. *Universe*, 5(9):200, 2019.
- [51] Wei-Chen Lin and William H. Kinney. Consistency of Tachyacoustic Cosmology with de Sitter Swampland Conjectures. *JCAP*, 10:038, 2019.
- [52] Richa Arya. Formation of Primordial Black Holes from Warm Inflation. *JCAP*, 09:042, 2020.
- [53] Mar Bastero-Gil and Marta Subías Díaz-Blanco. Gravity waves and primordial black holes in scalar warm little inflation. *JCAP*, 12(12):052, 2021.